ISSN1346-7832

独立行政法人港湾空港技術研究所

港湾空港技術研究所報告

REPORT OF THE PORT AND AIRPORT RESEARCH INSTITUTE

VOL.42 NO.2 June 2003

NAGASE,YOKOSUKA,JAPAN
INDEPENDENT ADMINISTRATIVE INSTITUTION,
PORT AND AIRPORT RESEARCH INSTITUTE

港湾空港技術研究所報告（REPORT OF PARI）
第42巻　第2号（Vol. 42, No. 2），2003年6月（June 2003）

目　　次（CONTENTS）

REPORT OF THE PORT AND
AIRPORT RESEARCH INSTITUTE
VOL.42, NO.2 (June 2003)

Greenbelt Tsunami Prevention in South-Pacific Region

Tetsuya HIRAISHI*
Kenji HARADA**

Synopsis

The South-Pacific region including Indonesia and Papua New Guinea (PNG) has suffered from so many tsunami disasters these days. Tsunami caused at the Sissano area, PNG in 1998 run up to 15m above sea level and killed more than 2000 residents. The north-east region in the Sulawessi island had a tsunami attack with the height of 2～4m and the regional costal houses were heavily damaged by run-up tsunami flow pressure. The fast evacuation from the coast after shaking is the most important regional countermeasure method to tsunami disaster. The regional meeting and lectures on tsunami mechanism have been held in the target areas since the 1998 PNG tsunami event. The elders and children have, however, the difficulty in evacuating from the shore in a few minutes. The warning for early evacuation is not given in case that the tsunami may be generated in the offshore far from shore.

The alternative countermeasure applying the hard barriers like coastal dikes and detached breakwaters becomes necessary in the coastal region with high tsunami risk. We propose the greenbelt barrier instead of the hard system like breakwaters because they cost high expense. The greenbelt is composed of the tropical trees with enough stability against tsunami pressure and it may be grown up in the residential vegetation of the coastal areas.

The two dimensional experiment was carried out in a tsunami channel for the evaluation of tsunami reduction effect. The chemical porous media was employed to reproduce the coastal forest in the experimental channel. The experimental results demonstrated that the greenbelt had the tsunami reduction effect similar to that in coastal dikes composed of wave energy dissipating blocks. The drag force coefficient in the greenbelt with porous media was derived from the experimental current and pressure data.

The numerical simulation in non-linear long wave model with the drag force terms was carried out to study on the greenbelt applicability in a practical topography. The 1998 PNG tsunami was employed for the target. The underwater landslide may be caused in the same time of earthquake shaking. The greenbelt 100m wide was installed along the shore in the Sissano region. The maximum tsunami run-up height on shore became smaller in the case with greenbelt countermeasure than in the case with no protection. The numerical test results demonstrated that the greenbelt with specified tropical trees was applicable as a sustainable tsunami prevention method in the South-Pacific region.

Key Words: tsunami prevention, greenbelt, sustainable method, hydraulic experiment, field survey

* Head of Wave Division, Marine Environment and Engineering Department
Nagase 3-1-1, Yokosuka, Kanagawa 239-0826, Japan
Phone: +81-46-844-5042, Fax: +81-46-841-3888, E-mail: hiraishi@pari.go.jp

** Former research student of Wave Division (Present, Assistant researcher, Disaster Prevention Research Institute, Kyoto University)

港湾技術研究所報告
第42巻第2号(2003.6)

グリーンベルトを用いた南太平洋地域の津波対策

平石哲也*・原田賢治**

要　旨

環太平洋地震帯の南縁に位置するインドネシアやパプアニューギニア地方は，従来から数々の地震被害とそれに伴う津波被害を受けてきた．その中でも1998年パプアニューギニア北岸のシッサノ地区を襲った津波は局所的に15mの遡上高を記録し，2000人の命を奪っている．また，2000年インドネシア東部スラウェシ島の津波は2-4mの高さにも係わらず，海岸の家屋をすべて流し，沿岸の家屋を破壊した．このような津波被害を軽減し，沿岸の居住区の安全性を高めるためには，地震と津波に関する知識を普及し，地元住民が地震後すみやかに避難できるような体制をつくることがまず重要である．

しかし，地震が沖合の海洋で発生し，沿岸では強い揺れを感じない場合や，子供，老人等の避難行動が迅速にとれない災害弱者を守る場合には，ソフトウエア的な対策だけでは不十分である．そのため，人口の集中が進む地区では，我が国で多く採用される防潮堤や防波堤の建設が強く望まれる．ただし，南太平洋地域は社会資本の蓄積が不十分で，高額な防潮堤等のハードウエアの整備は難しい．そこで，沿岸の環境整備にも有益で，地元住民の協力で簡単に整備できるグリーンベルトによる津波防災を提案した．グリーンベルトは高さ数mの幹と四方に広がる葉部を有する熱帯性の樹木林で，植樹により海岸部に育成する．

津波来襲時のグリーンベルトの効果を定量的に明らかにするために，1/50縮尺の模型を用いてグリーンベルトによる津波水位，津波流速，津波波圧の低減量を調べた..水流圧力の低減量で比較すると，グリーンベルトによる低減率は消波ブロックで製作された海岸堤防とほぼ同一であり，防潮堤や海岸堤防のハードウエアによる津波対策施設と同様の効果を期待できることが判明した．そこで，模型実験結果から導いたグリーンベルトの抗力係数を数値計算に用いて，1998年シッサノ地区津波を対象としてグリーンベルトの効果を定量的に調べた．その結果，10m四方の土地に20～30本の特定樹木を育成すると，樹木林がない場合に比較して最大津波高を1/2程度に低減できることがわかった．

キーワード：津波防災，グリーンベルト，南太平洋地域，水理模型実験，現地災害調査

* 海洋・水工部　波浪研究室長
〒239-0826　横須賀市長瀬３－１－１　港湾空港技術研究所
電話：046-844-5042,　Fax：046-841-3888,　E-mail：hiraiashi@pari.go.jp
**（前）海洋・水工部波浪研究室実習研究員，（現）京都大学防災研究所助手

CONTENTS

1. Introduction

The South-Pacific region including Indonesia and Papua New Guinea (PNG) has suffered so many tsunami disasters these days. Tsunami caused at the Sissano area, PNG in 1998 run up to 15m above sea level and killed more than 2000 residents. The northern east region in the Sulawesi island had a tsunami attack with the height of 2 ~ 4m and the regional costal houses were heavily damaged by run-up tsunami flow pressure. The fast evacuation from the coast after shaking is the most important regional countermeasure method to tsunami disaster. The regional meeting and lectures on tsunami mechanism have been held in the target areas since the 1998 PNG tsunami event. The elders and children have, however, the difficulty in evacuating from shore line in a few minutes. The warning for early evacuation is not done in case that the tsunami may be generated in the far offshore.

The alternative countermeasure applying the hard barriers like coastal dikes and detached breakwaters becomes necessary in the coastal region with high tsunami risk. We propose the greenbelt barrier instead of the hard system like breakwaters because they cost high expense. The greenbelt is composed of the tropical trees with enough stability against tsunami pressure and it may be grown up by the residential vegetation in the coastal areas.

The two dimensional experiment was carried out in a tsunami channel for the evaluation of tsunami reduction effect. The chemical porous media was employed to reproduce the coastal forest in the experimental channel. The experimental results demonstrated that the greenbelt had the tsunami reduction effect similar to that in a coastal dikes composed of wave energy dissipating blocks. The drag force coefficient in the greenbelt with porous media was derived from the experimental current and pressure data.

The numerical simulation in non-linear long wave model with the drag force terms was carried out to study on the greenbelt applicability in a practical topography. The 1998 PNG tsunami was employed for the target. The underwater landslide was assumed to be caused in the same time of earthquake shaking. The greenbelt 100m wide was installed along the shore line in the Sissano region. The maximum tsunami run-up height on shore became a half times smaller in the case with greenbelt countermeasure than in the case with no protection. The numerical test results demonstrated that the greenbelt with specified tropical trees was applicable as a sustainable tsunami prevention method in the South-Pacific region.

2. Tsunami disaster in Asia and Pacific region

2.1 Field survey in 2000 East-Sulawesi earthquake tsunami

Indonesia and Papua New Guinea located on the rim Pacific earthquake belt have suffered from many tsunami disasters. The occasional frequency of tsunami hazard becomes high these days. **Table 1** shows the recent history of tsunami hazard in the South Pacific Region. The tsunami survey team reported the highest run-up tsunami height became up to 15m in the Sissano sand spit located in the northern PNG (Hiraishi,2000). The number of suffered persons slightly varies in several survey reports. The number in the table obeys to the local community meeting (Hiraishi,2000).

The recent large tsunami hazard occurred in the Banggai Islands and Luwuk area located in the north-east Sulawesi in 2000. The author conducted field survey to obtain the origin of high tsunami risk in the target areas. The earthquake with Lichiter scale magnitude of 6.5 occurred on May 4, 2000 in the Sulawesi, Indonesia. **Figure 1** shows the location of epicenter and suffered areas. The tsunami damage became large in Luwuk city and Banggai island near from the epicenter. The high story buildings, bridges and local roads in Luwuk were damaged by strong shake. **Photograph 1** shows the fallen wall of a bank in the central area.

Table 1 Recent tsunami catalog in Indonesia and PNG

No.	Year	Affected Region	Ms	Run-up Height(m)	Human damage
1	1965	Seram,Molucca	7.5	4	71
2	1967	Tinambung,Sulawes	5.8	4	58
3	1968	Tambu,Sulawesi	7.4	10	200
4	1969	Majene,Sulawesi	6.9	10	64
5	1977	Sumba	8.0	15	189
6	1982	Larantuka	5.9	?	13
7	1992	Flores	7.5	26	2100
8	1994	Banyuwangi,Java	6.8	14	208
9	1996	Palu,Sulawesi	7.7	6	8
10	1996	Biak,Irian Jaya	8.0	12	160
11	1998	Taliabu,Molucca	7.7	3	34
12	1998	Sissano,PNG	7.1	15	1236

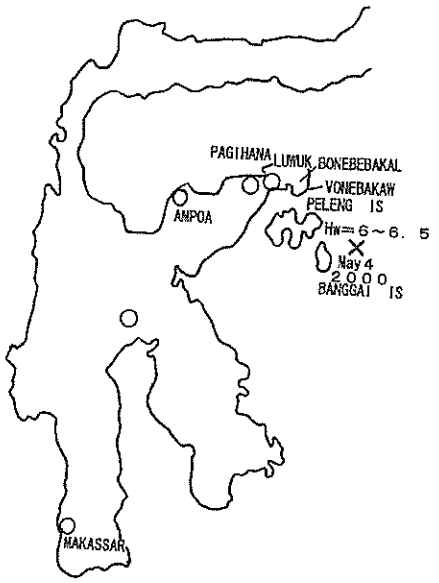

Figure 1 Location of 2000 Sulawesi earthquake

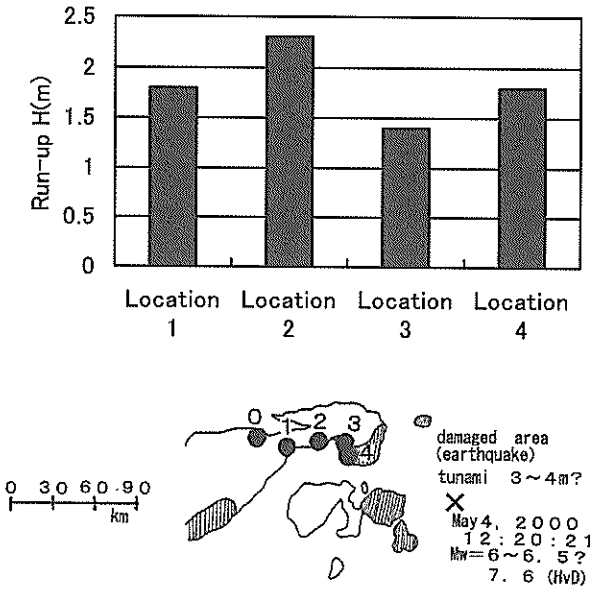

Figure 2 Inundated area and tsunami run-up height

Photograph 1 Damaged bank building in Luwuk (2000)

We carried out field survey of tsunami run-up height along the coast facing to Banggai straight. **Figure 2** shows the area inundated by tsunami. The map is derived from the original survey map of Luwuk city office (Luwuk City Office, 2000). The run-up height was obtained from the interview to local people. We measured the run-up heights in the main land because of difficulty in landing the island*. The run-up height became about 2m. The local authority said the tsunami height in Banggai island was about 4m. Forty-four people were lost by earthquake shake and tsunami. The major part was lost by tsunami flow in the island area.

Photograph 2 shows the housing damages in coastal shore. The fishermen houses in the coast were damaged

(1) Collapse of coastal house

(2) Swashed maritime houses

Photograph 2 Housing damage in Luwuk coast (2000)

by tsunami attack. The house wall was collapsed by wave pressure. The maritime houses located on sea were completely swashed as shown in Photograph 2 (2). The piers in sea represent the supporter of house.

* We carried out the field survey on September, 2000. The survey time was limited by the social disturbance.

2.2 Origin of disaster integration

The tsunami hazard in the Pacific area usually become worse than in Japan where tidal barriers and coastal dikes have the effect against the maximum tsunami force. No damage was not observed in port facilities in case of the 1996 Hokkaido Toho-Oki Earthquake tsunami which had the run up height similar to that of 2000 Sulawesi tsunami.

The reason why the damage by tsunami attack becomes larger in the South Pacific region is mainly supposed to be in the weakness of housing facility on the first line. The maritime houses built on sea are supported in thin wooden piles so the facilities on upper deck may be easily swashed by tsunami flow. Such maritime style houses are widely employed even on shore in the north PNG. **Photograph 3** shows the typical maritime house in PNG.

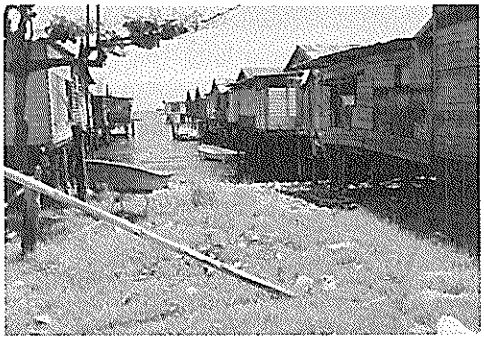

Photograph 3 Image of maritime house (2003, Port Moresby)

Even on shore, the houses are usually framed using thin wooden walls. The wooden houses have been easily destroyed in tsunami swash. The collapsed parts may cause attacks to people in water. We suggested the possibility of relocation of maritime houses and proposed the implementation of buffer zone for reduction of tsunami flow pressure. **Figure 3** shows the image of relocation of maritime houses and implementation of coastal forest shading the housing area from offshore (Hiraishi, 2000).

The relocation to the innermost land may cause the inconvenience to fishing on sea. The distance from the shore should be set in several hundreds meters from shore line. A sustainable buffer zone like coastal forest is suitable as tsunami disaster prevention method in the target areas if the buffer has enough effect to reduce tsunami height and pressure.

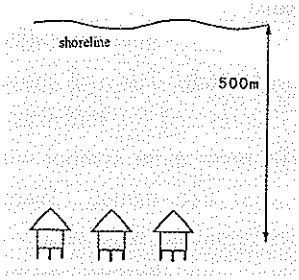

(1) Relocation

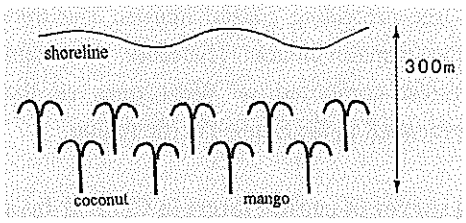

(2) Greenbelt

Figure 3 Tsunami mitigation image in coast

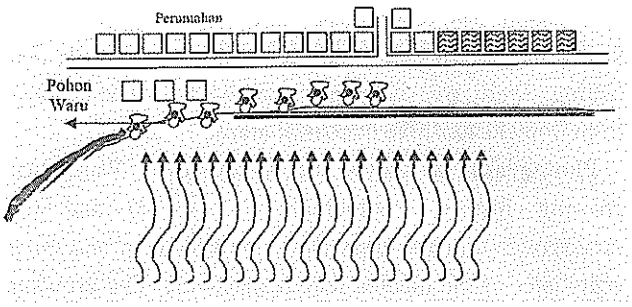

Figure 4 Protection effect of Waru tree (Amri, 2000)

2.3 Proposal of greenbelt prevention method

Greenbelt should be implemented between shore line and inland housing area to reduce tsunami flow pressure in the allowable level for wooden houses. The coastal forest consisting greenbelt is chosen from the tropical trees like coconuts, mango and mangrove. The mangrove has the wide root and dense leaf so it suitable to reduce the tidal surge. We experimentally demonstrated that the chemical sheet with porosity the same to that of the mangrove decreased the height of solitary wave in channel (Harada et al., 2002).

Mangrove is, however, not suitable in sandy beaches where the local residence mainly habitats. Mangrove is grown up only in the estuary area near to river mouth. The coconuts are widely grown up in the tropical areas. The many coconuts, however, were fallen down and rooted up in the Sissano area in 2000. So coconuts are not strong enough to endure the tsunami flow pressure.

Alternative plants were proposed in a local meeting. **Figure 4** shows the damage map in a village attacked by the 2000 Sulawesi tsunami. The map shows the swashed houses in hatched areas and the remained houses in the white squares. The rectangular symbol with black circle indicates the coastal tree named "Waru" The house behind Waru trees remained without any damage while the houses without any barrier at the front were completely swashed. The map supposes the effectiveness of Waru tree protecting coastal houses. The trees were stable after tsunami attack. Therefore we propose the coastal forest composed of Waru trees as the most suitable greenbelt in the South-Pacific region.

2.4 Field survey of coastal forest in Central Java

We carried out the field tour to investigate the applicability of Waru tree as greenbelt. Waru tree is one kind of zelkova trees and widely grown up in the central Java Island. The south coasts near from Yogyakarta are facing the Indian Ocean and suitable to swimming and fishing. Waru tree is mainly planted to make shadow from tropical sunshine in coastal areas.

Photograph 4 shows the situation of Waru tree growing history. Photograph 4 (1), (2) and (3) corresponds to a few days later, one year later and three years later of the planted date respectively. The growing speed of the tree is very rapid and the tree becomes several meters high in several years.

Figure 5 shows the annual variation of averaged height and diameter of trunk derived from field survey. The year of each tree were evaluated from the interview to local residents. The life time of tree is about 10years and distance between each tree were 3 to 5m. The coastal forest composed of Waru trees is supposed to be sustainable system in residential areas and to be easily planted by local community.

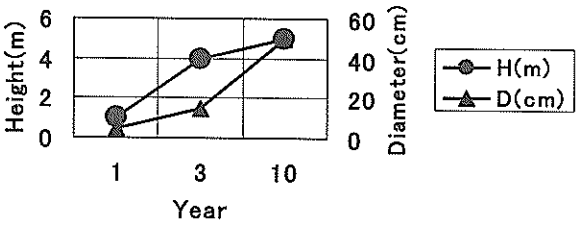

Figure 5 Annual variation of Waru height and diameter

(1) a few days later

(2) one year later

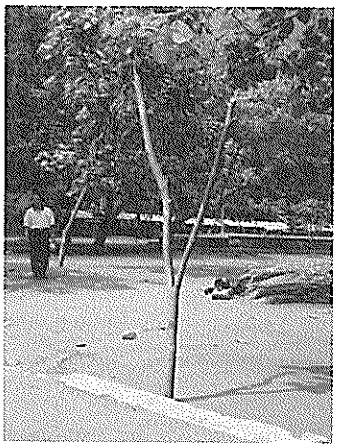

(3) three years later

Photograph 4 Growing of Waru tree

3. Experimental modeling of greenbelt prevention zone

3.1 Experimental set-up

We conducted the wave channel experiment to investigate the tsunami reduction effect of greenbelt. **Figure 6** shows the cross and plane of wave channel. The channel has a vacuum tower pumping water. The water level inside tower becomes up to 2m high when the air pressure in tower decrease. The water mass instantaneously falls down and generates the solitary waves when the air valves mechanically opens.

Figure 7 shows the wave profile obtained at the

observation points of channel. The wave height is changed according to the number of opened valves. The channel has shallow part with uniform depth and the 1/50 slope onshore site. The greenbelt model is installed at sore line and the wave profile, current velocity and wave pressure were measured at the foot step of slope (M.P.1), in the front of greenbelt (M.P.2), in the backside of greenbelt (M.P.3) and in the backward 30cm apart from greenbelt (M.P.4) respectively.

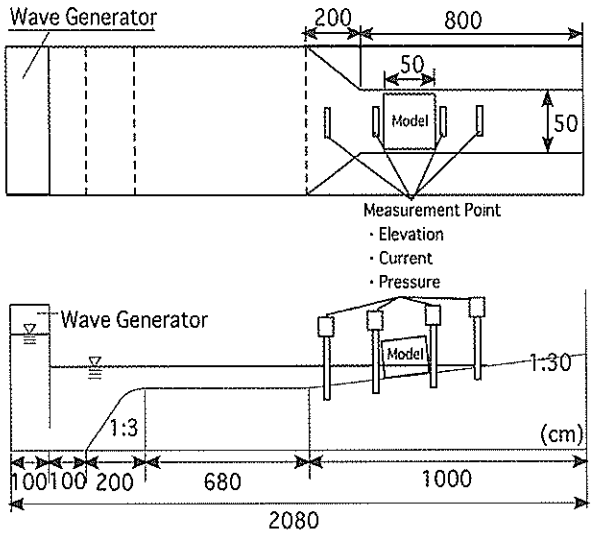

(a) Experimental Set-up

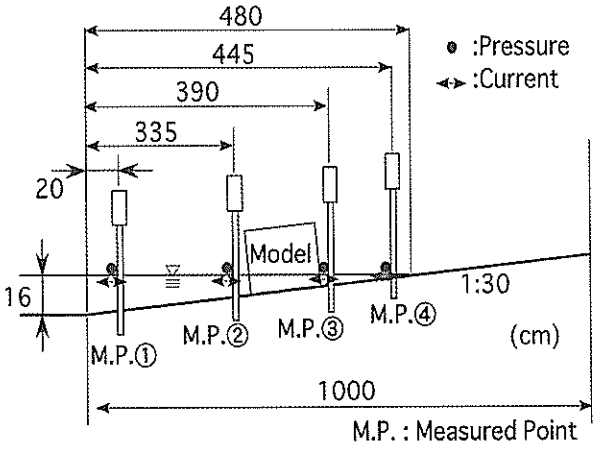

(b) Measuring points

Figure 6 Cross and plane section of channel

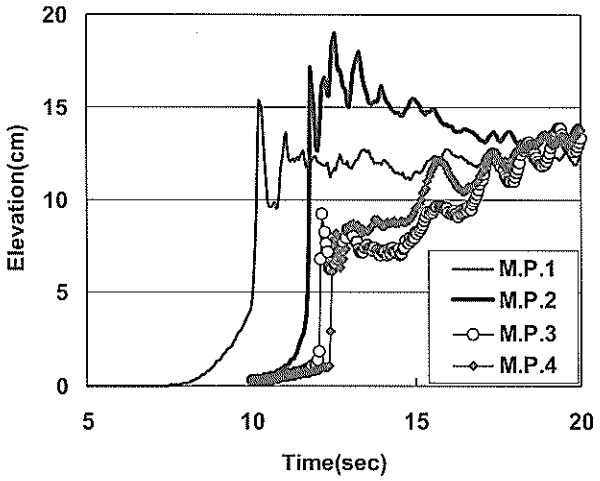

Figure 7 Observed wave profile

The porous media composed from the chemical wave absorbing sheet was employed as the part of leaf and root. The plastic column with 1cm diameter was applied to reproduce the trunk part of greenbelt. The width of greenbelt was 50cm at the base line. **Figure 8** (1) shows the cross section of greenbelt and arrangement of trunk. The number of opened valves was two and five in the experimental cases. We evaluate the forest density by the total porosity of greenbelt model. The total porosity of model is calculated as the volume rate of plastic and chemical material to greenbelt frame.

The experimental results in greenbelt model may be influenced in the scale effect in test and tsunami profile. We suppose the different material test is necessary to compare the measured data in different porosity. We carried out the similar tsunami test in the different material. **Figure 8** (2)-(5) shows the different tsunami protection facilities for the comparison with greenbelt effect. The size of each facility is same to the frame of greenbelt. Fig.8(2) shows the greenbelt with uniform porosity. The porosity is determined in the porosity of chemical material. Fig.8(3) shows the coastal dike model with wave dissipating blocks. Fig.8(4) shows the coastal breakwater with rubbles. This type breakwater is widely employed in the local areas of Indonesia. Fig.8(5) shows tsunami prevention houses that are implemented in a Japanese coastal town.

The wave profile, current velocity and wave pressure were obtained at M.P.2, M.P.3 and M.P.4 in the tsunami channel for case of (S1) coastal tree model, (S2) uniform greenbelt model, (S3) wave dissipating block

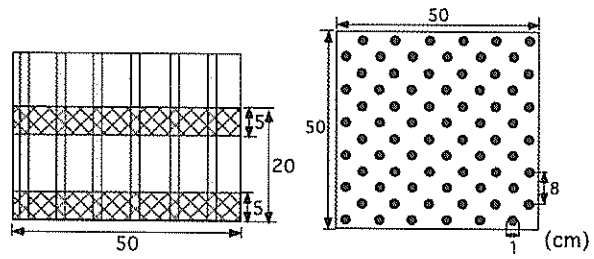

(1) Coastal forest model (S1)

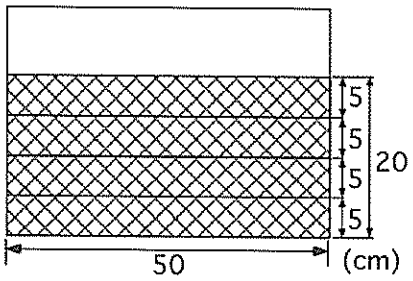

(2) Uniform greenbelt model (S2)

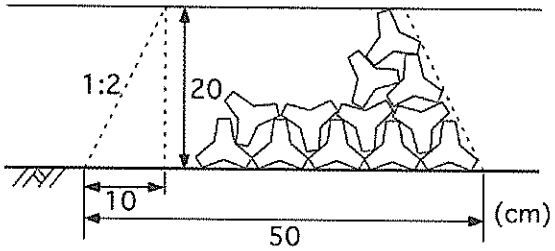

(3) Wave dissipating block dike (S3)

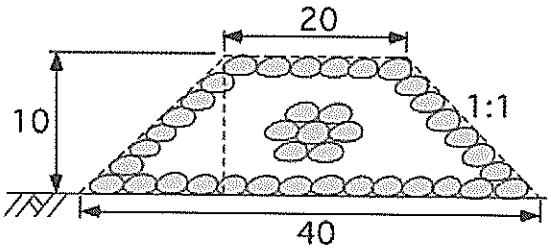

(4) Rubble breakwater (S4)

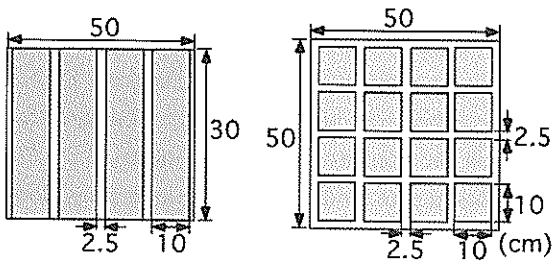

(5) House model (S5)

Figure 8 Tsunami protection facility

dike, (S4) rubble breakwater and (S5) coastal houses. The averaged porosity Sv of each structure is 0.97, 0.97, 0.75, 0.38 and 0.36 for S1, S2, S3, S4 and S5 respectively. The sampling time of wave data was 20ms.

3.2 Experimental results

Figure 9 shows the comparison of measured wave profile, current velocity and wave pressure for case without any barrier and with greenbelt (S2). Fig.9 (1), (2) and (3) corresponds to the variation of wave profile, current velocity and wave pressure respectively. In the figures, the black and white line represents the tsunami variation in channel with and without greenbelt respectively.

The measured tsunami height above initial water level becomes larger in case with greenbelt than without greenbelt because of reflected tsunami waves at the front point (M.P.2). In the backside points, M.P.3 and M.P.4, the measured tsunami has no major peak and maximum height becomes about 40% smaller in the greenbelt effect.

The maximum current velocity decreases in the backward of greenbelt. The tsunami pressure in channel with no barrier becomes two times larger at the greenbelt front point than in coast with greenbelt. The situation becomes reverse in the backside of greenbelt as shown in Fig.9 (3). The maximum tsunami pressure behind greenbelt protection becomes a half of that in channel with no barrier.

The greenbelt may increase the tsunami height at the offshore side by reflection wave from that. The water level, current velocity and wave pressure become smaller in the backside of greenbelt. Especially, the reduction of tsunami pressure by greenbelt becomes remarkable.

Figure 10 shows the comparison of tsunami reduction effect in the different type coastal barriers. In the figures, the horizontal axis represents the distance from the foot of uniform slope. The location of greenbelt corresponds to the area between the second and third plots location from the left side in the figures. The indicated values represent the rate of measured data with coastal structures (S1~5) to the data obtained in channel without coastal barriers. Fig.10 (1), (2) and (3) represents the dimensionless tsunami height, maximum current velocity and maximum wave pressure respectively.

The tsunami height is uniform at the offshore point for all structure cases but increases at the measurement point in the front face of coastal structures. The dimensionless tsunami height rapidly decreases through the coastal porous barriers. The height slightly increases in the far backside of the porous barriers.

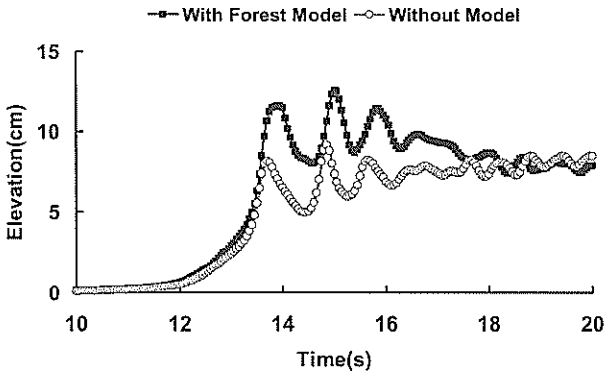

(a) at M.P.2

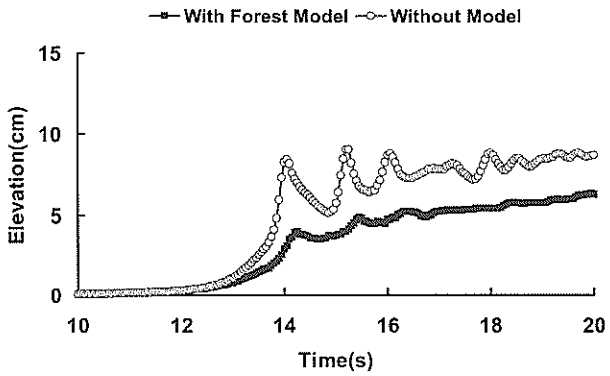

(b) at M.P.3

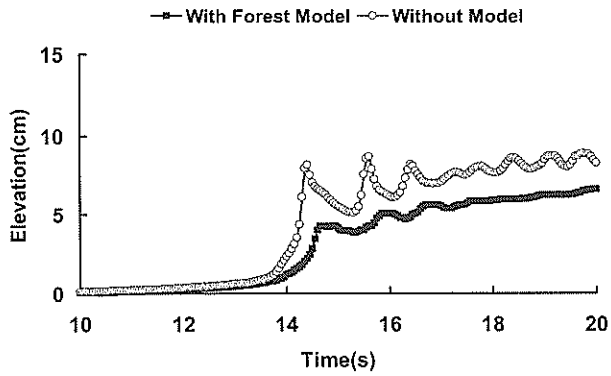

(c) at M.P.4

(1) Measured tsunami profile

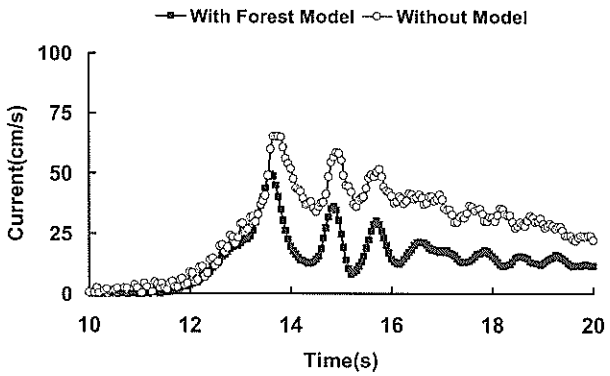

(a) at M.P.2

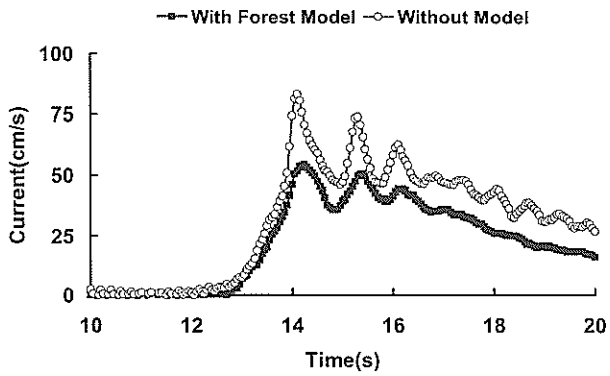

(b) at M.P.3

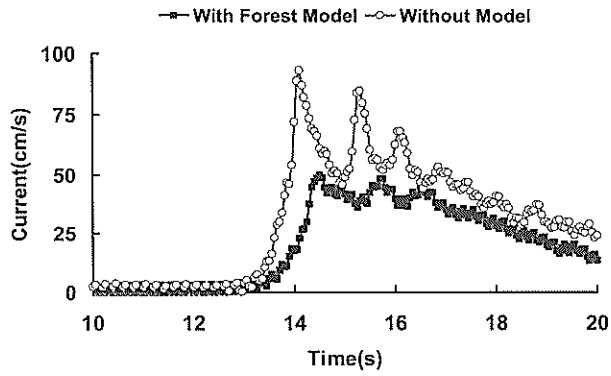

(c) at M.P.4

(2) Measured flow velocity

Figure 9 Variation of measured hydraulic data with and without greenbelt (1)

The current velocity gradually decreases when the distance increases. The reflection from the porous barriers may cause tiny influence to the variation of current velocity. The current velocity for house case (S5) shows the major increase at M.P.3 because the current breathing from the small gap of houses.

The maximum tsunami pressure also becomes larger in case with the porous barriers than in case without any barriers at the front of the barrier position. The dimensionless wave pressure behind the porous barriers become below 1.0 for all types. The dimensionless pressure behind porous barriers becomes the minimum in case of the coastal breakwater.

The tsunami power is usually evaluated in the flow

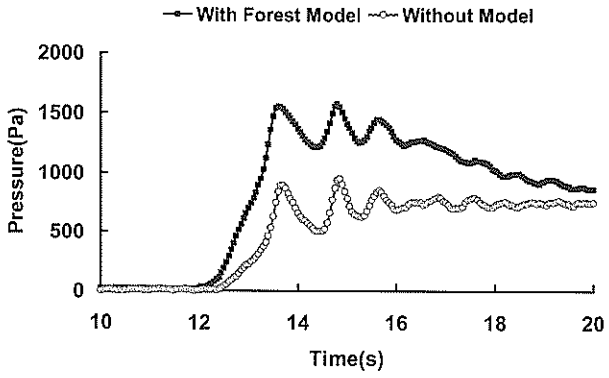

(a) at M.P.2

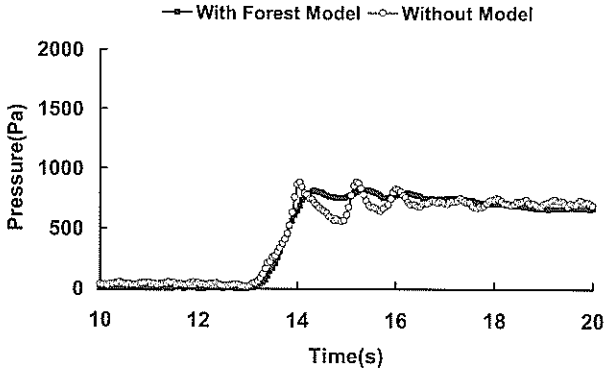

(b) at M.P.3

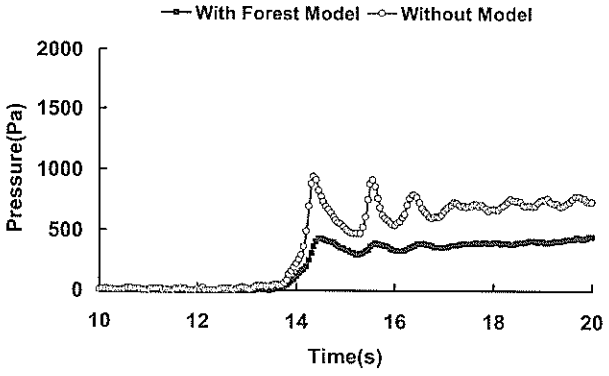

(c) at M.P.4

(3) Measure wave pressure

Figure 9 Variation of measured hydraulic data with and without greenbelt (2)

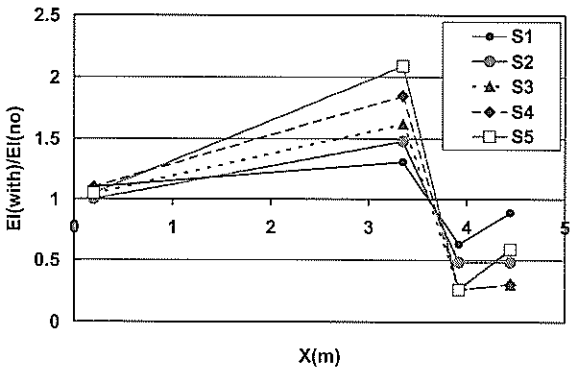

(1) Tsunami height

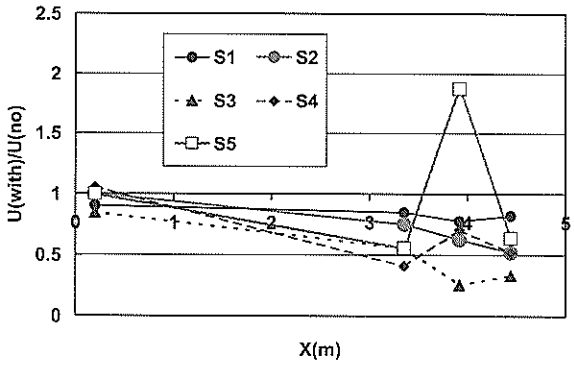

(2) Tsunami flow velocity

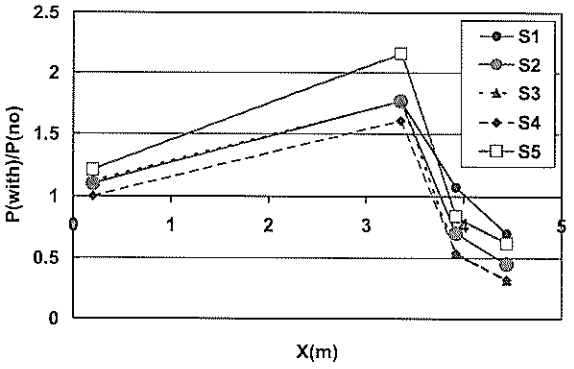

(3) Tsunami pressure

Figure 10 Variation of dimensionless measured tsunami height, current and pressure in various porous barriers

pressure defined by $\rho u^2 \eta$ (ρ :water density, u: current velocity, η :water level above ground level).

Figure 11 shows the comparison of dimensionless maximum flow pressure measured in the backward points M.P.3 and M.P.4. In the figure N.V. indicates the number of opened valves. The dimensionless flow pressure becomes below 1.0 for all cases except of the rigid house case at M.P.3. The reason why the flow pressure becomes larger than 1.0 is supposed to be the effect of fast breathing current from house gaps located between the model piers.

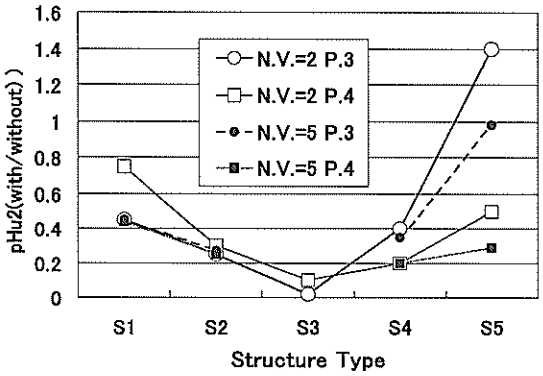

Figure 11 Comparison of maximum flow pressure for various coastal facility

The dimensionless flow pressure does not change for tsunami size according to the opened valve number and it becomes the minimum in case of the wave dissipating block barrier (S3). The second best barrier is S4 (rubble mound) or uniform greenbelt. In the target model with trunk and leaf part (S1), the dimensionless flow pressure becomes slightly larger than in the case of rubble mound breakwaters. The dimensionless flow pressure becomes 0.4 for the both tsunami profiles generated in N.V.=2 and 5. The size of experimental target greenbelt is 50m in the width of prototype. The tsunami reduction effect of greenbelt is smaller than the breakwater with wave dissipating blocks. However, the reduction effect of tsunami by greenbelt becomes similar to the rubble breakwater with similar size. Therefore the greenbelt prevention method may be applicable to a sustainable tsunami reduction system alternative to the hard breakwater in the tropical coastal zone.

The tsunami reduction mechanism in porous barriers is complicated and the influence of overflow and wave overtopping may give wide variation to the flow pattern behind the barriers. The reduction effect becomes different between in the tree model (S1) and in the uniform forest model (S2) even if the both model has the same porosity Sv=0.97. However the difference between the both models becomes about 10% in the maximum dimensionless wave pressures. We suppose the tsunami reduction effect of greenbelt barrier is approximately represented by the averaged porous rate in the total mass of greenbelt frame.

The tsunami pressure reduction in the porous barrier is represented as the drag resistance proportion to (tsunami flow velocity)^2 and the inertia resistance proportion to flow acceleration. The measured pressure gap between the front and back side of greenbelt WF is approximately defined in the following equation.

$$WF = \frac{1}{2} C_D \rho A_O u|u| + C_M \rho \frac{V_O}{V} \frac{\partial u}{\partial t} \quad (1)$$

where C_D and C_M represents the drag and inertia coefficient. The symbol of A_O and V_O represents the effective projection area and body mass of greenbelt under water surface. The volume V indicates the volume under water occupied in the outside frame of greenbelt. Fig.9 (2) mentioned before shows the time dependent variation of current velocity is small and the current velocity in greenbelt becomes almost uniform except of the initial time when surge front approaches to the greenbelt front. Therefore the pressure decreasing in greenbelt is mainly caused in the drag resistance.

We employed the uniform greenbelt model to approximately evaluate the tsunami pressure decrease in the drag and inertia terms. One of the authors (Harada and Imamura, 2001) conducted the additional series of tsunami test using the porous sheet indicated in Fig.8 (2). He measured the variation of tsunami current velocity and pressure using the porous medias with different porosity. The experimental current velocity and tsunami pressure measured in the time-region when the current velocity becomes almost stable. The inertia resistance is negligible in the stable current condition. Therefore, the drag coefficient is directly derived from the pressure gradient.

Figure 12 shows the derived relationship of determined drag coefficient C_D and the porous rate Vo/V.

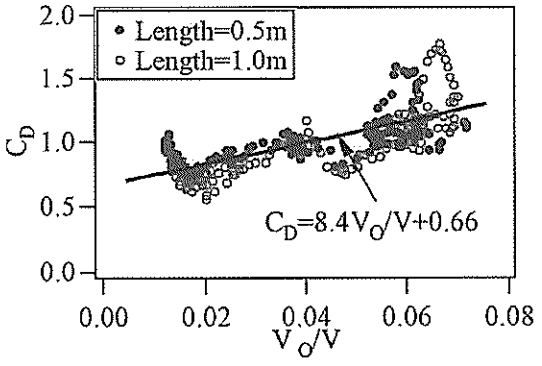

Figure 12 Relationship of C_D and Vo/V

The inertia coefficient is determined to minimize the gap of estimated and measured water pressure at the initial wave front. The drag coefficient C_D and inertia coefficient C_M is approximately evaluated in the following.

$$C_D = 8.4Vo/V+0.66$$
$$C_M=1.7 \quad (2)$$

4. Application of greenbelt to practical coast model

4.1 Evaluation of pressure reduction

We carried out a numerical simulation for tsunami generated in the Sissano lagoon, PNG, 1998 (Hiraishi, 2000). We proposed the submarine landslide as one major source to generate the devastated tsunami. The shape of submarine landslide was assumed at first as the impractical vertical hole at sea bottom. We developed the circular sliding model as a practical landslide and verified the model by reproducing the 1768 Yaeyama earthquake tsunami (Hiraishi et al. 2001). The submarine landslide may often cause in the shallow water area in Indonesia and PNG coast where the soft clay is thickly accumulated on steep sea bed. The submarine landslide may be generated even in slight shaking of small earthquakes and cause locally the large tsunami run-up. The evacuation after shaking is difficult because of lack of feeling the strong earthquake on shore. We evaluated the greenbelt applicability in a practical coast resembling the Sissano coast, PNG.

The non-linear long wave propagation model is employed in the tsunami simulation. The momentum equation in x-direction on the inundated area is expressed in the following equation.

$$\frac{\partial M}{\partial t}+\frac{\partial}{\partial x}\left(\frac{M^2}{D}\right)+gD\frac{\partial \eta}{\partial x}+\frac{gn^2M|M|}{D^{7/3}}$$
$$+\frac{C_D}{2}\frac{A_O}{\Delta X\Delta Y}\frac{M|M|}{D^2}+C_M\frac{V_O}{V}\frac{\partial M}{\partial t}=0 \quad (3)$$

The indication M, D, n represents the flow flux in x-direction, total water depth and the Manning roughness on sea bed and land. The first, second, third and force term in the equation is originally included in the momentum equation. The tsunami reduction effect of greenbelt is represented as the drag resistance and inertia resistance in the fifth and sixth term in the equation (3). The inertia resistance term should be included in the second dispersion term but the spatial gradient of flow flux is negligible in the tsunami case. The resistance terms are directly computed in the equation (3) with the drag part proportion to averaged flow velocity's square and the inertia term proportion to the flow flux acceleration.

We assume the coastal tree as the structure consisting the thin column and porous leaf. **Figure 13** shows the modeled tropical tree with a rigid trunk with the diameter D' and leaf part with porosity Sv=0.97. The height of trunk is assumed to be 5m according to the field survey. The diameter D' is 1.0m. The height and width of leaf part $H2$ is the same and $H2$ is 5m in the simulation. The effective projection area and volume of leaf part is derived from the porosity Sv. The width of greenbelt B on land is fixed in the simulation. We changed the spatial density of greenbelt in employing the tree number in a specified area. The greenbelt applicability is evaluated in the number of trees in a unit area. The effective projection area and volume of trunk part is expressed in the following;

$$A_1 = h_D\left(D'\frac{N}{100}\Delta x\Delta y\right)$$
$$V_1 = h_D\left(\pi\frac{D'^2}{4}\frac{N}{100}\Delta x\Delta y\right) \quad (4)$$

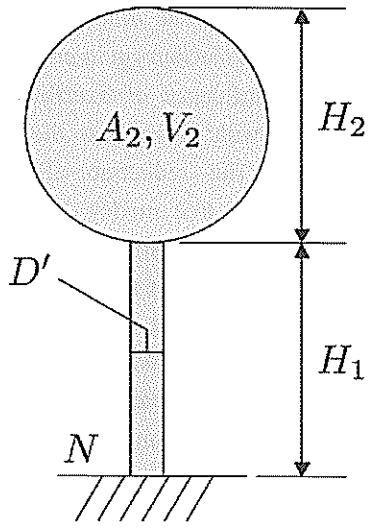

Figure 13 Image of modeled unit tree in greenbelt

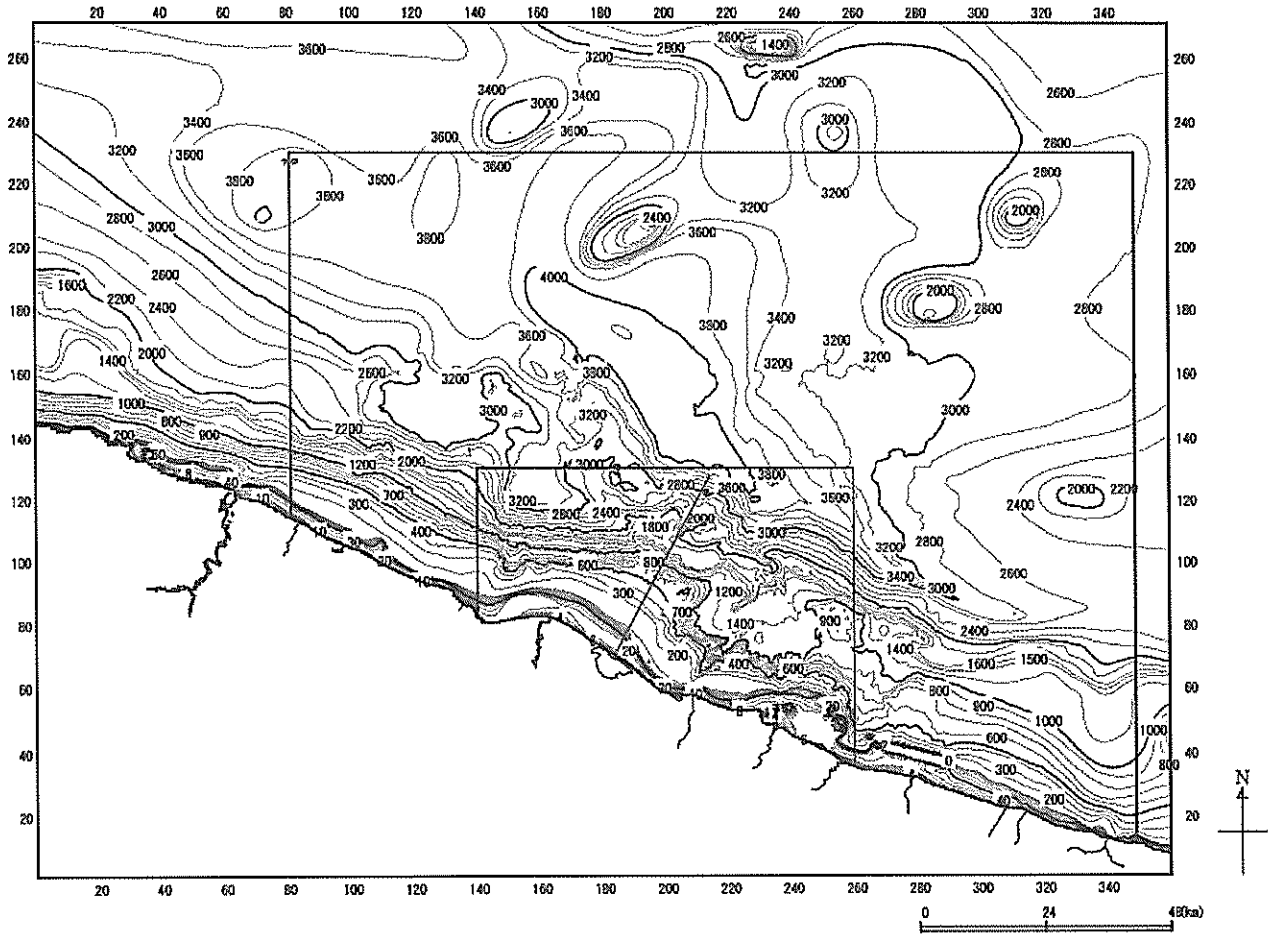

Figure 14 Topography and location of Sissano area
(The line normal to shore corresponds to the cross section in Figure 15)

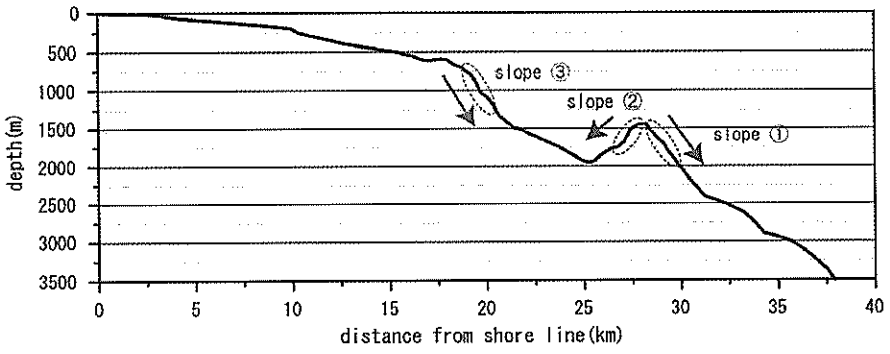

Figure 15 Cross section of submarine landslide line

where, h_D indicates the inundated water depth on land. The number N represents the tree number in the unit area of 100m^2. In the computation, the tree number was N=0 to N=30. In case of N=0, no greenbelt is implemented in the shore area. In case of N=30, the tree is planted with a gap of 2-3m in cross grid.

4.2 Tsunami reproduction of 1998 PNG disaster

Figure 14 shows the plane topography in the Sissano coast, PNG. The Sissano area consists the sand spits and lagoon and has steep sea bed offshore. **Figure 15** shows the cross section of submarine bathymetry offshore side of the Sissano coast. We assumed the land slide might

cause on the steep slope indicated in the number (1), (2), (3). The circular slide model (Hiraishi et al., 2001) was adopted on each submarine slope and the most unstable failure face was determined. The location of supposed main land fault is referred to Hiraishi (2000).

Figure 16 shows the initial tsunami profile observed at the offshore point 600m apart from the shore. The submarine landslide is supposed to be generated on the slope(3) at the same time to earthquake shaking. The first peak of tsunami profile is caused in the landslide and its height becomes much larger than the height of tsunami generated in the main earthquake shaking. The initial tsunami profile may be changed in the duration of sliding. The duration of sliding is indicated in τ in the figure. The tsunami peak increases when the duration decreases. We employed τ =15s as the minimum time duration. As the shorter duration is impractical to the large landslide, we adopted τ =15s as the landslide duration.

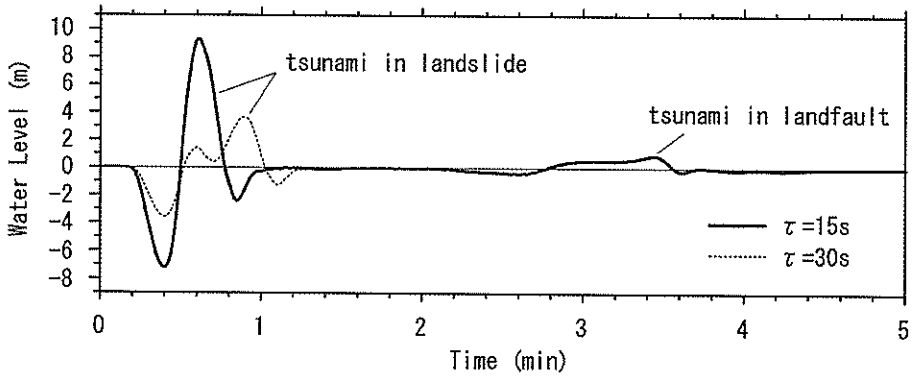

Figure 16 Initial tsunami profile generated in landslide(3) and earthquake fault

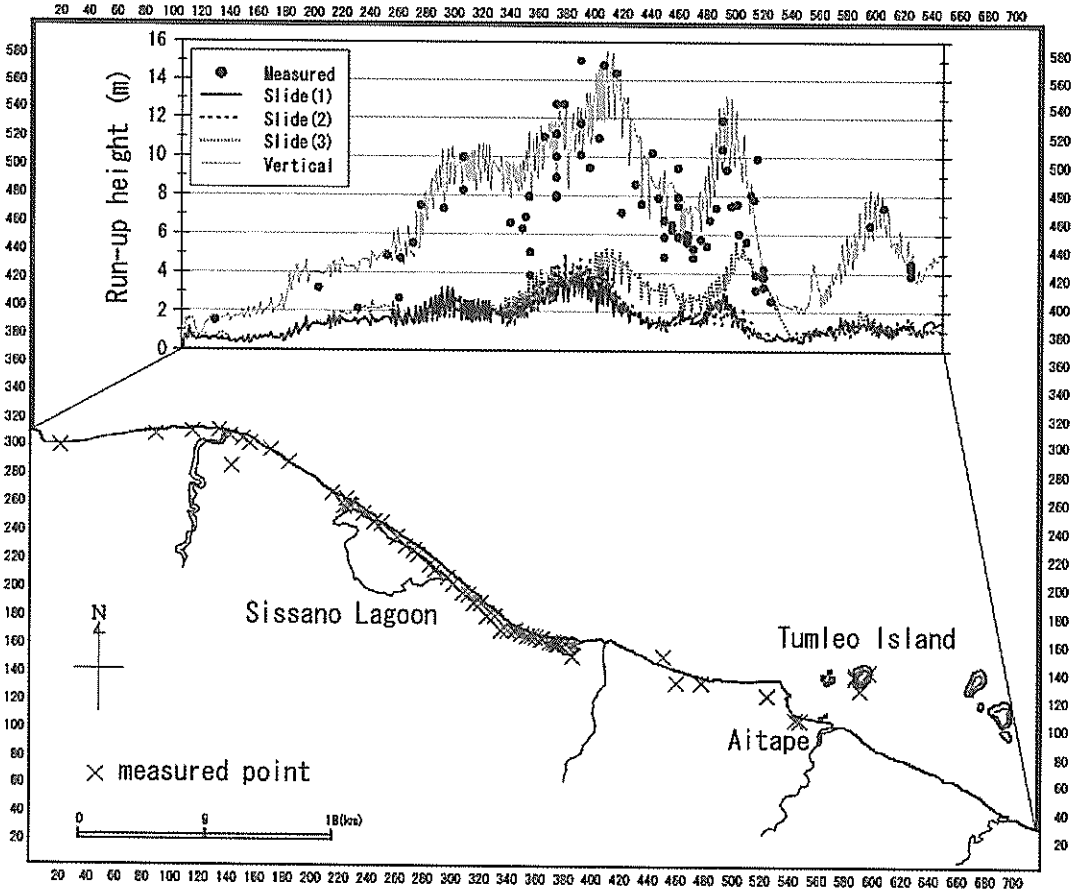

Figure 17 Measured and estimated tsunami run-up height along the Sissano coast

Figure 17 shows the spatial variation of maximum tsunami run up height of the devastated coast. The measured tsunami run-up height becomes more than 15m on the sand spit of Sissano. The estimated tsunami run-up height with the landslide on slope(3) becomes up to 5m at the maximum. The spatial distribution of estimated and measured tsunami shows the similar two peaks. The location where the run-up peak appears is the same in the both of measured and estimated tsunami.

Therefore we applied the landslide model on slope(3) that represents the highest tsunami height in the computation as the tsunami model reproducing 1998 PNG tsunami. We suppose the error of maximum tsunami run-up height between the observation and simulation coming from the local refraction of long wave, the splash to high coconuts tree, high order dispersion of run-up wave and the unknown factor in landslide mechanism. The detail study including the geological survey is necessary to fully understanding of 1998 PNG tsunami.

The circular type landslide model is supposed to be suitable to reproduce the maritime landslide tsunami. However the tsunami run-up height computed in the model becomes much smaller than the measured run-up height in PNG. Hiraishi (2000) has proposed the vertical sliding model as the initial mass variation to approximate the submarine landslide. The thin rigid line in Fig.17 shows the distribution of tsunami run-up height in the vertical slide mode. The run-up height computed in the later model agrees well with the measured height because the sliding mass was adjusted in the trial computation. We applied the vertical sliding model to reproduce the tsunami that attacked the Sissano coast in 1998. The detail study is necessary to develop a new model to explain the 1998 PNG tsunami mechanism with more accuracy.

4.3 Numerical prediction of greenbelt applicability

We employed the tsunami model generated in the vertical landslide (Hiraishi, 2000) as the target of tsunami disaster prevention. The cross section on land is assumed to be uniform. **Figure 18** shows the standard cross section of beach derived from the field survey (Matsutomi et al., 1999). The low hill with 3m high is located behind the shore. The hosing area was located at the backside of low hill. We assume the greenbelt is implemented between the shore and coastal hill. The width of greenbelt is 100m and it is set along shore.

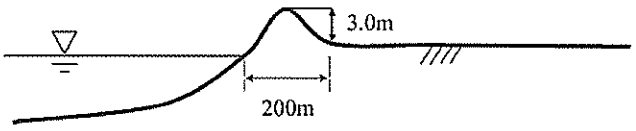

Figure 18 Cross section of standard beach in Sissano

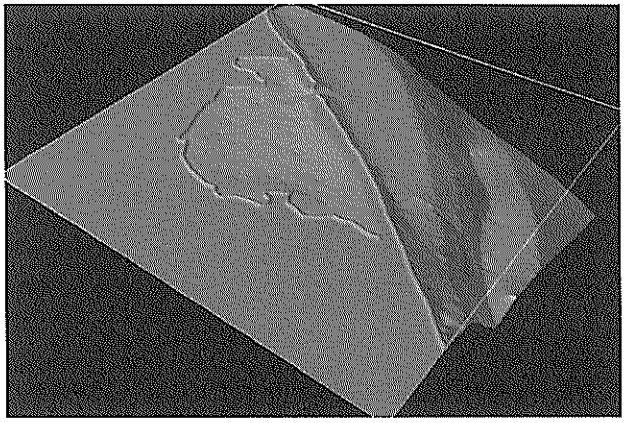

Figure 19 Topography of shallow water and low land in Sissano lagoon and vicinity

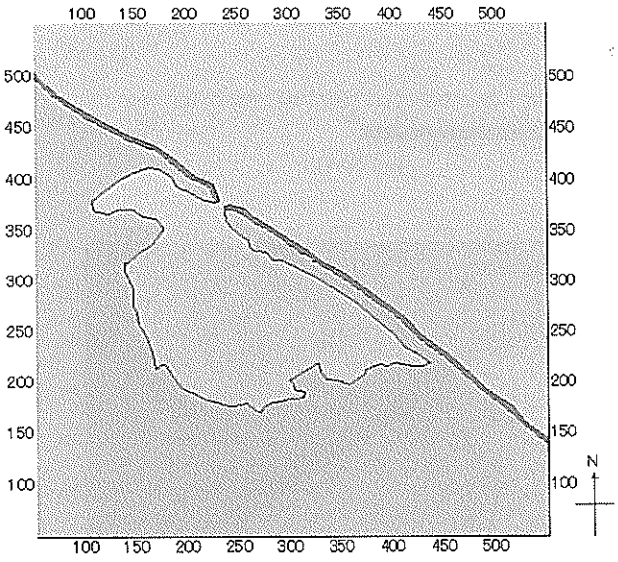

Figure 20 Plane map of Sissano lagoon area and greenbelt

Figure 19 shows the bird view map of target area where the tsunami run-up is simulated with fine meshes of 25m grids. The greenbelt is installed to protect the whole region included the sand spits and lagoon. Figure 14 mentioned before shows the plane map of

computation area for tsunami run-up.

The greenbelt is installed along shore. The width of greenbelt is 100m. **Figure 20** shows the location of greenbelt in the finest grid area. The tsunami approaches to shore and attacks directly to greenbelt. The dark line in the figure represents the greenbelt set between the shore and low coastal hill. The width of greenbelt is uniform in the computation area. The density of greenbelt varies for the number of planted tree N in a unit square area (10m x 10m).

The tsunami computation was done for the case of N=0, 10, 20 and 30. The maximum inundated water depth and tsunami height during tsunami simulation was compared for the evaluation of greenbelt effect. The wave height in shallow water region becomes larger in the case of greenbelt installation than in the case of no greenbelt. The reflected wave and flow may cause the increase of tsunami height in shallow water situated in the front side of greenbelt.

Figure 21 shows the variation of maximum tsunami surface elevation in the finest grid area for the greenbelt density. The unit in the figure is meter.

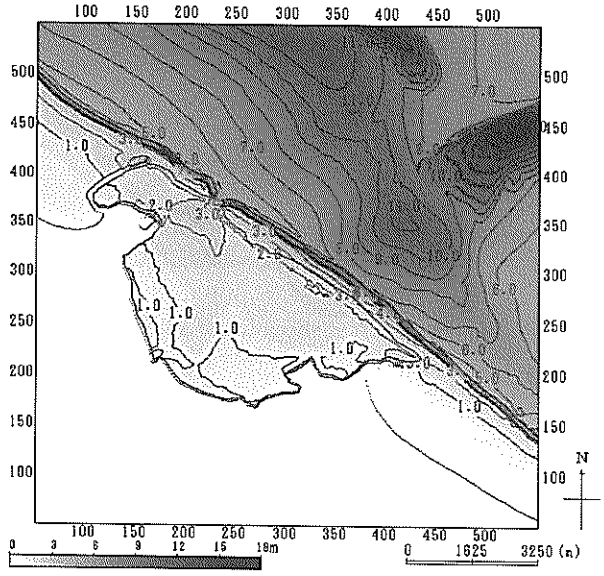

(1) N=0

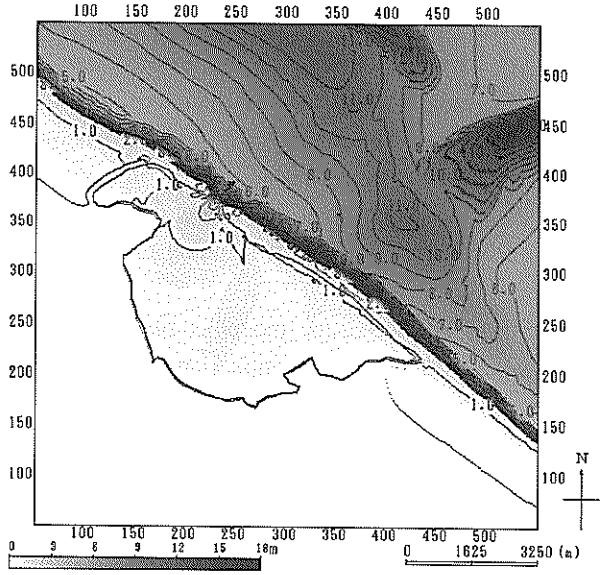

(2) N=10

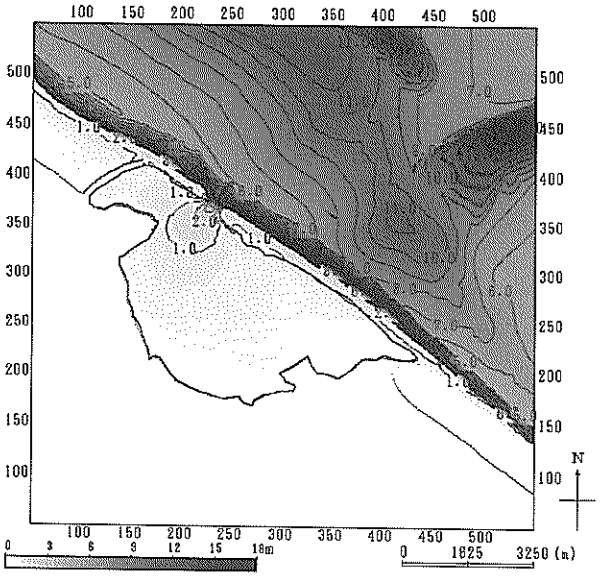

(3) N=20

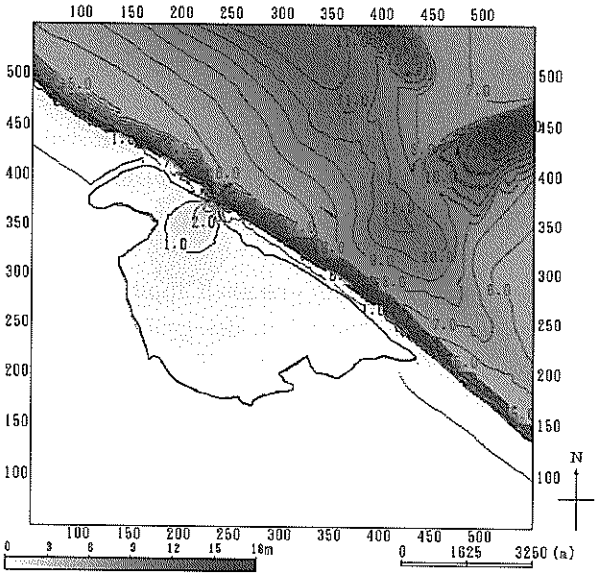

(4) N=30

Figure 21 Variation of maximum tsunami surface elevation for greenbelt density

For the case of no protection (N=0), the maximum surface elevation in front of the west sand spit covering the Sissano lagoon becomes about 8.0-7.0m. The height increases when the number of tree N increases in case of N=10 and N=20. The tsunami wave reflected in the greenbelt may give the influence to the tsunami wave height in the shallow coast. The maximum surface elevation decreases in case of N=30 compared with the cases of N=10 and 20. The dense greenbelt may be effective to reduce the reflection coefficient of tsunami wave affecting the vicinity coast. We should make the greenbelt with density enough to prevent the occurrence of remarkable reflection tsunami.

Figure 22 shows the comparison of the maximum inundated water depth on land and the maximum inundated area. The maximum inundated water depth becomes slightly larger in case of N=10 than in N=0. The greenbelt reduces the total tsunami energy on land but it may cause the water accumulation by the decrease of flow velocity on land. The inundated depth and area becomes remarkably small in case of N=30 compared with the case of no protection.

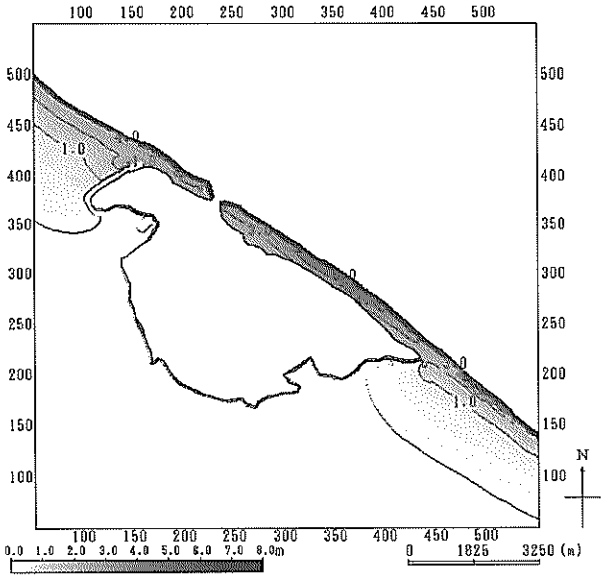

(1) N=0

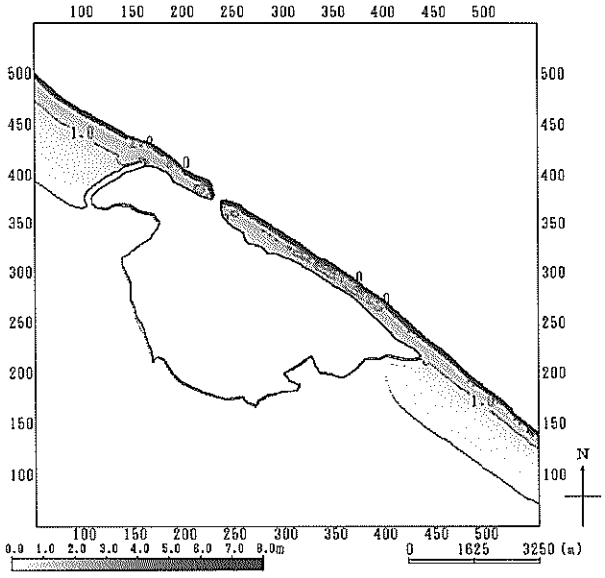

(2) N=10

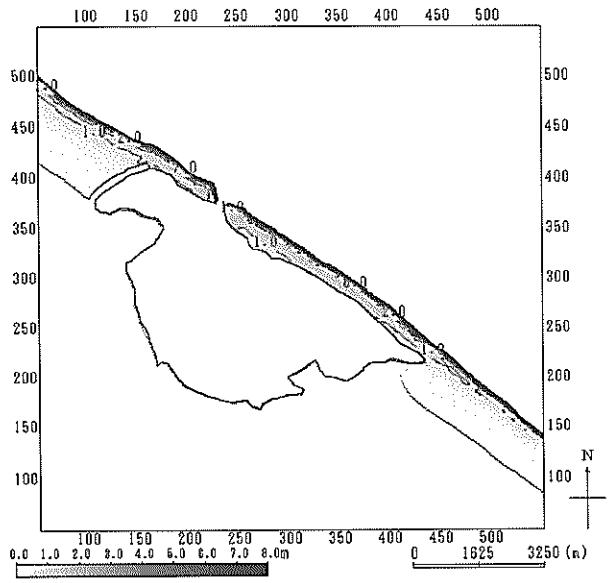

(3) N=20

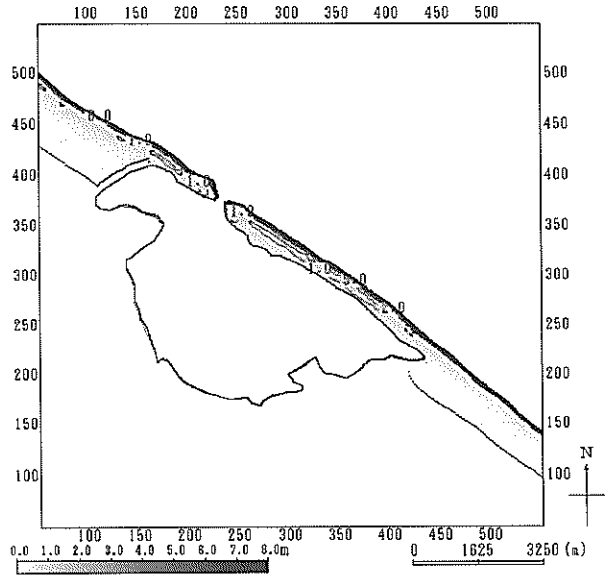

(4) N=30

Figure 22 Comparison of inundated water depth estimated in various greenbelt density

The density of greenbelt should be larger than the density represented in N=30 in order to perfectly prevent the tsunami inundation even in the gigantic tsunami observed in PNG.

The density represented in N=30 corresponds to the situation that two or three trees are planted in 10m distance. The gap between each Waru tree derived from the field survey was about 5m. We may make the additional plantation to complete the greenbelt satisfying the target density.

The effect of greenbelt should be evaluated in the reduction rate of the maximum tsunami flow pressure behind of the greenbelt line. We compared the tsunami profile in the specified points on the cross section indicated in Fig.18. Hiraishi et al. (2000) has suggested the wooden houses may be heavily damaged when the flow pressure becomes larger than 10^5 N/m from the field survey in a flooded area in storm surge.

Figure 23 shows the location of measurement points on sea and land. In the figure the colored area represents the inundated land area in tsunami run-up. The inundated area decreases as the greenbelt density indicated in N increases. At P01, P02 and P03, the both sides of front and backside are expressed in the profile figures.

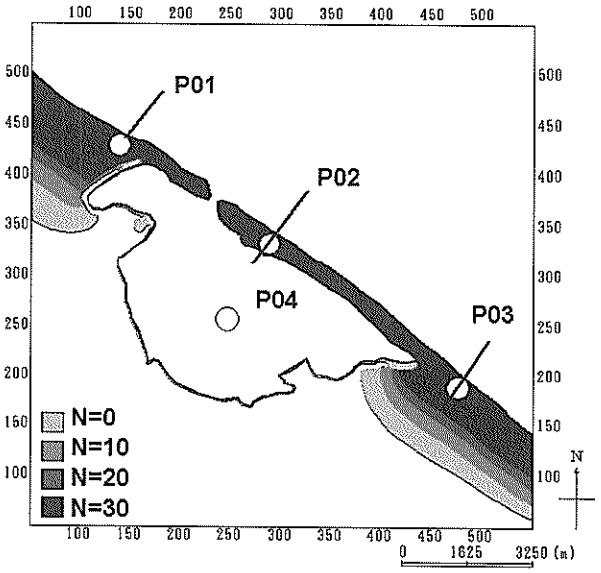

Figure 23 Measurement point for tsunami profile

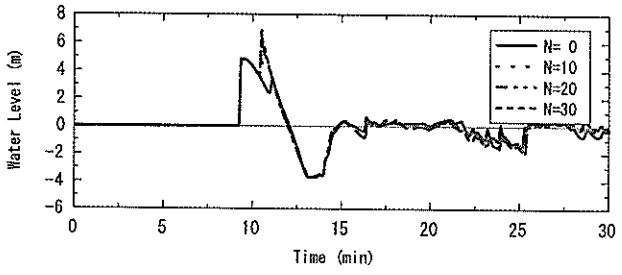

(a) front side

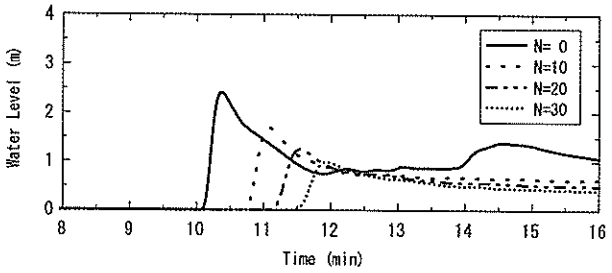

(b) back side

(1) P01

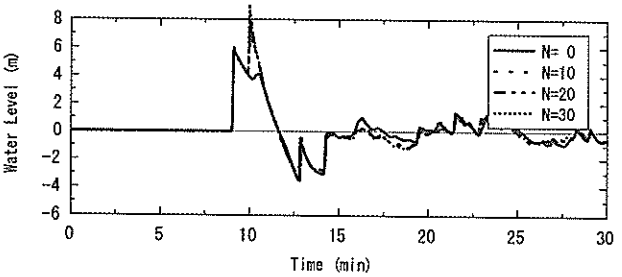

(a) front side

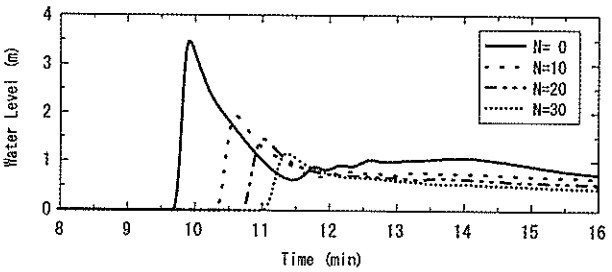

(b) back side

(2) P02

Figure 24 ···continued

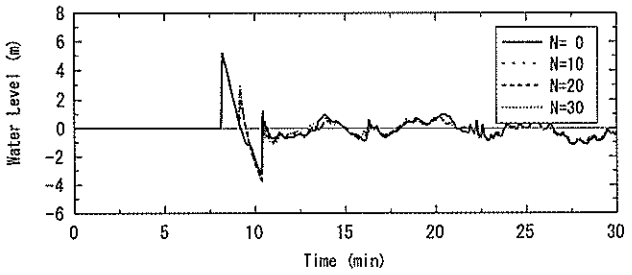

(a) front side

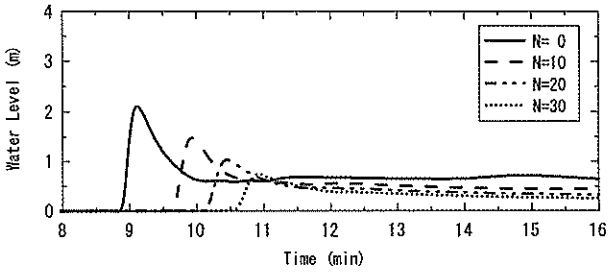

(b) back side

(3) P03

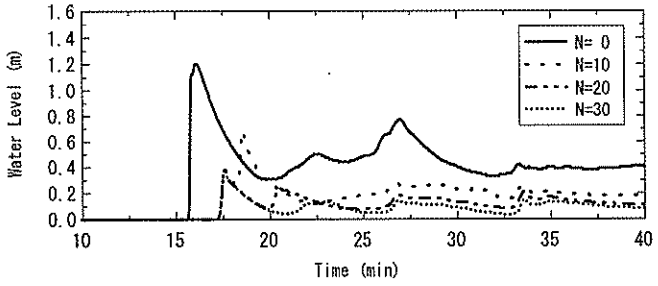

(4) P04

Figure 24 Tsunami profile estimated in specified point for various forest density

Figure 24 shows the comparison of tsunami wave profile measured at each measurement location indicated in Fig.23. The datum line is set on the land level. In the points P01, P02 and P03, the tsunami profile is expressed in the both of front and back side of greenbelt. Fig.24 (1) shows the tsunami profile in the front (a) and back (b) side of P01. The peak height in profiles measured at the front side increases as the number of tree in a unit area N increases because of effect in tsunami wave reflection.

The tsunami profile in the backside (Fig.24(1)-b) demonstrates the remarkable reduction of tsunami peak height in the dense greenbelt. The peak height decreases as the density increases. The arrival time of first tsunami wave also is delayed in the effect of greenbelt. The dense greenbelt may be effective to delay the tsunami arrival time and to reduce the peak height.

In the other measurement points P02 and P03, the variation of tsunami profile becomes similar to that in P01. The location P02 represents the measurement point on the sand spit where the evacuation is difficult. The peak height of tsunami profile becomes about 30% in the case of N=30 compared with the case of no protection.

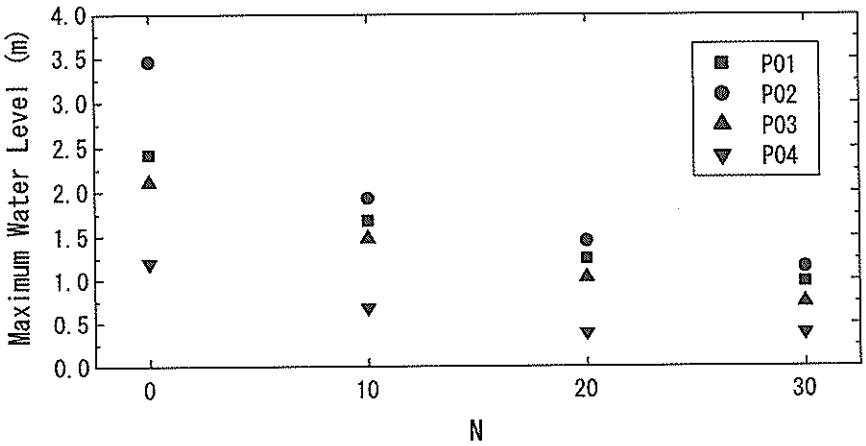

Figure 25 Variation of maximum water level on land for greenbelt density

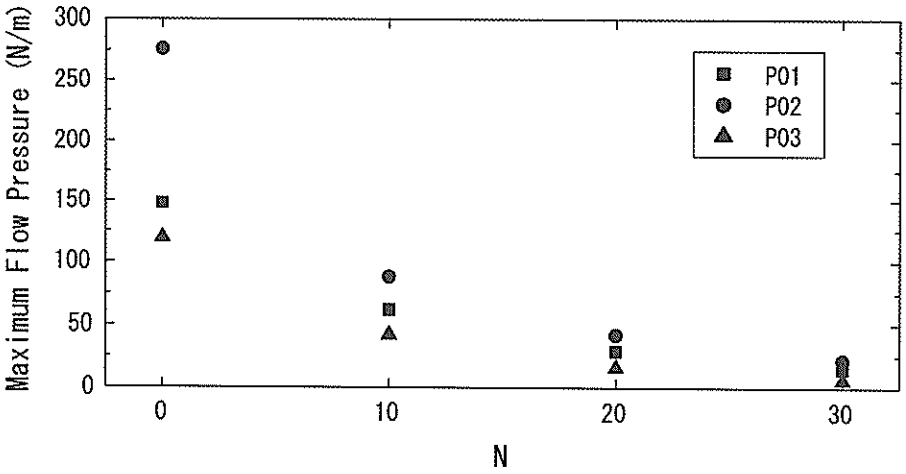

Figure 26 Variation of maximum flow pressure estimated on ground for N

Figure 25 shows the variation of the maximum tsunami flow pressure at each measurement point for the density of greenbelt. The maximum tsunami flow pressure decreases as the number of tree N increases. The decreasing rate is more remarkable when the maximum tsunami flow pressure for N=0 becomes larger. The vegetation of greenbelt is effective to reduce the tsunami peak level on the inundated areas.

We estimated the tsunami flow pressure as the production of tsunami flow velocity with the surface elevation at every time steps. **Figure 26** shows the variation of maximum flow pressure computed at the backside in each measurement point. The flow pressure is evaluated in the points on land, P01, P02 and P03.

The maximum tsunami flow pressure in case without any protection becomes the largest in P02. The flow pressure decreases remarkablg when the greenbelt is installed. For example the value becomes 1/2.5 in case of N=10 compared with no protection case. In case of N=30, the maximum flow pressure becomes smaller than 10% of the initial pressure. Fig.26 demonstrates the dense greenbelt is quite effective to reduce the flow pressure. When we obtain the allowable flow pressure level in the target residential area, we are able to design the necessary width and density of greenbelt in the computation model.

The greenbelt applicability to tsunami risk reduction system in the target areas is confirmed in numerical simulation results.

5. Conclusions

We conducted the field survey on possibility of greenbelt tsunami prevention at first. We continuously carried out the experimental study to evaluate the effect of greenbelt by comparison with the model test for different type coastal protection methods. We finally presented the applicability of greenbelt using a model coast with high tsunami risk in a two dimensional tsunami simulation.

The major results of survey are as follows;

1) A tropical tree called "Waru" is suitable to the greenbelt component because it has protected the coastal houses from the tsunami attack in a practical field.

2) The growing up speed of Waru tree is very fast and it may form the greenbelt in several years.

3) Tsunami water level, flow velocity and pressure measured in a tsunami channel becomes smaller for case of the porous barrier representing greenbelt than for case of no protection.

4) The reduction rate of flow pressure in the greenbelt becomes similar to that in the coastal dike composed of rubbles.

5) The tsunami simulation with the submarine landslide model reproduces the tsunami run-up height distribution in the Sissano-coast ,PNG with the allowable accuracy.

6) The inundated water area in tsunami run-up decreases when the density of installed greenbelt increases.

7) The greenbelt effect is remarkable in the comparison of flow velocity on the inundated land.

8) The greenbelt 100m wide along the coast is applicable to the sustainable tsunami risk management system in the South Pacific region.

(Received on February 14, 2003)

Acknowledgement

We deeply appreciate to Prof. Fumihiko Imamura, Disaster Control Research Center, Graduate School of Engineering, Tohoku University for his suggestion to tsunami prevention method in the Asia and Pacific region. We express sincere thanks to Mr. Hiroyuki Iwase, ECOH Co. Ltd., for his help us in carrying out the numerical simulation of tsunami propagation.

References

Amri S. (2002) : Housing and environmental damages due to 4 May 2000 Banggai Earthquake in Cetral Sulawesi Province of Indonesia, Proc. International Workshop on Tsunami Risk and Its Reduction in the Asia-Pasific Region, Bandung, Indonesia, Session 1.

Harada K. and F. Imamura (2001) : Experimental study on the resistance by mangrobe under the unsteady flow, Proc. of the first Asian and Pacific Coastal Engineering Conference, Dalian, China, Vol.2, pp.975-984.

Harada K. H.Latief and F.Imamura (2002) : Effect on reducing tsunami by the green belt and costal permeable structure, Proc. International Workshop on Tsunami Risk and Its Reduction in the Asia-Pasific Region, Bandung, Indonesia, Session 4.

Hiraishi T. (2000) : Characteristics of Aitape tsunami in 1998 Papua New Guinea, Report of the Port and Harbour Research Institute, Vol.39, No.4, pp.3-23.

Hiraishi T.,K.Hirayama and H.Kawai (2000) : A study on wave-overtopping by Typhoon No.9918, Technical Note of the Port and Harbour Research Institute, No.972, 19p.

Hiraishi,T., H.Shibaki and N.Hara (2001) : Numerical simulation of Meiwa-Yaeyama Earthquake Tsunami in landslide model with circular rupture, Proc. of Coastal Engineering, JSCE, Vol.48, pp.351-355,(in Japanese).

Luwuk City Office (2000) : Deskripsi Penanganan Kerusakan Pasca Gempa Bumi Yang Terjadi Di Kabupaten Banggai, 12p,(Indonesian).

Matsutomi, H., Y. Kawata, N. Shuto, Y. Tsuji, K. Fujima, F. Imamura, M. Matsuyama, T. Takahashi, N. Maki and S. Han (1999) : Flow strength on land and damage of the 1998 Papua New Guinea earthquake Tsunami, Proc. of Coastal Engineering, JSCE, Vol.48, pp.351-355,(in Japanese).

List of Symbols

A_O	:	Effective projection area of greenbelt underwater
A_2	:	Effective projection area in leaf part
C_D	:	Drag force coefficient
C_M	:	Inertia force coefficient
D	:	Total water depth
D'	:	Diameter of tree trunk
H_1	:	Height of trunk part
H_2	:	Height of leaf part
H_D	:	Inundated water depth
M	:	Mass flux in x-direction
N	:	Number of tree in 10m square
N.V.	:	Number of opened valve in wave channel
p	:	Tsunami pressure
S_V	:	Porosity of greenbelt and permeable structure
u	:	Tsunami flow velocity
V	:	Volume of water
V_O	:	Effective body mass of greenbelt under water
η	:	Water level
ρ	:	Water density

港湾空港技術研究所報告（REPORT OF PARI）
第42巻　第2号（Vol. 42, No. 2），2003年6月（June 2003）

目　　次（CONTENTS）